ELSEVIER

Physica C 356 (2001) 97–106

PHYSICA C

www.elsevier.nl/locate/physc

Rhenium effect in the formation and stability of $HgCaO_2$ and $Hg_{1-x}Re_xBa_2Ca_2Cu_3O_{8+\delta}$ superconductor

A.G. Cunha [a,b,*], M.T.D. Orlando [a,b], K.M.B. Alves [a], L.G. Martinez [c], F.G. Emmerich [a], E. Baggio-Saitovitch [b]

[a] *Departamento de Física, Universidade Federal do Espírito Santo, 29060-900 Vitória-ES, Brazil*
[b] *Centro Brasileiro de Pesquisas Físicas, Rua Dr. Xavier Siguad 150-Urca, 22290-180 Rio de Janeiro-RJ, Brazil*
[c] *Instituto de Pesquisas Energeticas e Nucleares, Campus USP, 05508-900 São Paulo-SP, Brazil*

Received 9 September 2000; received in revised form 22 December 2000; accepted 2 January 2001

Abstract

Using a novel technique (thermobaric analysis or TBA) to measure in situ the pressure in quartz tubes, we have investigated the influence of Hg and Re_x content in the range $0.00 \leqslant x \leqslant 0.25$ on the formation and stability of $HgCaO_2$. Moreover the competition between the synthesis of $HgCaO_2$ and of the superconductor $Hg_{1-x}Re_xBa_2Ca_2Cu_3O_{8+\delta}$ (Hg,Re)-1223 was investigated. The pressure determination has enabled us to obtain all thermodynamic parameters such as the enthalpy $\Delta_d H^0$, entropy $\Delta_d S^0$ and the Gibbs free energy $\Delta_d G^0$ and follow the decomposition reactions by monitoring the pressure behavior. This possibility of pressure measurements has also allowed us to acquire a better knowledge on the effects of Re substitution in the formation of (Hg,Re)-1223. The TBA technique has also permitted us to minimize the $HgCaO_2$ impurity content and hence to improve the quality of the ceramic (Hg,Re)-1223 superconductor.

PACS: 74.25.Bt; 74.25.Dw; 74.72.Gr
Keywords: Synthesis of (Hg,Re)-1223; $HgCaO_2$; Thermobaric analysis; Pressure measurements

1. Introduction

The formation reactions of $HgBa_2Ca_{n-1}Cu_nO_y$ ($n = 1, 2, 3, \ldots$) are not completely established yet. The superconductor synthesis is very sensitive to atmospheric CO_2 and moist, which requires the handling of samples in controlled atmosphere to avoid exposure to air. It is possible to synthesize the pure phase at elevated pressures in the order of GPa [1,2] or by substituting mercury with higher-valence cations [3–7], such as Bi, Pb and transition elements as Re.

The Re substitution makes possible to work at normal pressures without a controlled atmosphere [8], which improves the phase stability of Hg12(n−1)n. In order to perform the solid–gas reaction, the sealed quartz tube technique has been used, and the total pressure produced by $Hg_{(g)}$ and $O_{2(g)}$ inside the quartz capsule is one of the most important synthesis parameters to stabilize the $n = 3$ phase [9,10]. The total pressure and the ratio P_{Hg}/P_{O_2} have influenced the competition between

* Corresponding author. Address: Departamento de Física, Universidade Federal do Espírito Santo, 29060-900 Vitória-ES, Brazil.
E-mail address: elisa@cbpf.br (A.G. Cunha).

0921-4534/01/$ - see front matter
PII: S0921-4534(01)00089-2

Hg12($n-1$)n for $n > 1$ and the $HgCaO_2$ synthesis. This binary oxide has been the most difficult impurity to eliminate, frequently remaining in the final product.

In this work we have studied the $HgCaO_2$ formation by replacing HgO with $(ReO_2)_x$ in the range $0 \leqslant x \leqslant 0.25$, and its competition with the superconductor synthesis $Hg_{1-x}Re_xBa_2Ca_2Cu_3O_{8+\delta}$ (Hg,Re)-1223. To do this, it was used a recently developed thermobaric analysis technique (TBA) [10–12], which has become a very useful tool to analyze gas–solid chemical reactions. This new technique uses a measuring device that is connected to the sealed quartz tube. The possibility of recording in situ the total pressure opens a new direct and non-destructive way that allows us to evaluate the thermodynamic parameters such as the enthalpy $\Delta_d H^0$ and entropy $\Delta_d S^0$.

2. Experimental

2.1. Preparation of $HgCaO_2$

In order to study the effect of Re on the reaction of $HgCaO_2$, the powders were prepared with different $(HgO)_{1-x}$:$(ReO_2)_x$:(CaO) ratio mixture ($x = 0.00$, 0.05, 0.10, 0.15, 0.18, 0.20 and 0.25), with HgO (99%, Aldrich), ReO_2 (99.9%, Aldrich) and CaO (99.9%, Aldrich). The later was previously calcinated at 1000°C for 15 h to assure the elimination of carbonates. The mixtures were homogenized in an agate mortar inside a glove box filled with nitrogen (99.5%) and pelletized uniaxially under 0.3 GPa. The resulting compact samples, with masses around 0.360 g, were inserted in the quartz tube of the thermobaric analyzer and sealed under vacuum (10^{-2} Torr). The samples were heated with a rate of 60°C/h up to 860°C, were hold for 1 h at the maximum temperature and then were cooled to room temperature at a rate of 60°C/h.

2.2. Preparation of $Hg_{1-x}Re_xBa_2Ca_2Cu_3O_{8+\delta}$

Five syntheses of the ceramic superconductors $Hg_{1-x}Re_xBa_2Ca_2Cu_3O_{8+\delta}$ were performed using the thermobaric analyzer previously calibrated. Sample #1 does not contain Re, and samples #2, #3, #4 and #5 have $x = 0.15$, 0.18, 0.18 and 0.25 respectively.

Initially, $Ba_2Ca_2Cu_3O_x$ (99.9%, Praxair) was annealed at 930°C in an oxygen flow for 15 h to assure the complete elimination of carbonates. Then the $Ba_2Ca_2Cu_3O_{7+\delta}$ and ReO_2 (99.9%, Aldrich) powders were weighted in the molar ratio for each sample [8], homogenized in an agate mortar and pelletized uniaxially under 0.5 GPa. The obtained pellets were annealed at 850°C in an oxygen flow for 12 h, subsequently homogenized, compacted and annealed again at 930°C in an oxygen flow for 15 h. This three-step process was performed to assure a homogeneous distribution of Re in the sample and elimination of carbonates in the obtained polyphasic precursor.

The precursors for samples #1 and #2 were annealed again at 930°C in an argon flow for 15 h. This procedure is used to reduce the excess of oxygen in the precursor. Then the precursors were then mixed with HgO (99, Aldrich) in the nominal stoichiometric quantity. The resulting powders were finally homogenized, pelletized under 0.5 GPa, in a rectangular form, wrapped with a gold foil and inserted in the quartz tube of the thermobaric analyzer with 87 mg of $Hg_{(l)}$. For sample #1 ($m_s = 3.423$ g, ff $= 0.64$ g/cm^3, $m_{Au} = 1.255$ g) the thermal treatment was carried out with a heating rate of 300°C/h up to 787°C, 120°C/h to 894°C, holding this temperature for 0.1 h, and −120°C/h to 865°C, holding this temperature for 10 h. The sample was then cooled under a rate of 120°C/h until room temperature was reached. The ff was defined [11] as filling factor and is the ratio between the sample mass and the internal volume of the TBA device. For sample #2 ($m = 3.791$ g, ff $= 0.58$ g/cm^3, $m_{Au} = 1.213$ g), the thermal treatment was carried out with a heating rate of 300°C/h up to 730°C, 120°C/h to 875°C, holding this temperature for 0.1 h, −120°C/h to 864°C, holding this temperature for 10 h and the cooling rate was 120°C/h down to room temperature.

For sample #3, after the initial treatment, the gas flow was blended with 90% argon and 10% of oxygen and the sample was annealed again at 930°C for 12 h. This precursor was then mixed

with HgO (99%, Aldrich) in a nominal stoichiometric quantity. The resulting powder was finally homogenized, pelletized, ($m = 3.380$ g, ff = 0.58 g/cm^3), wrapped with a gold foil ($m_{Au} = 2.118$ g) and inserted with 93 mg of $Hg_{(l)}$ in the quartz tube of the thermobaric analyzer. The thermal treatment was carried out with a heating rate of 300°C/h up to 700°C, 120°C/h to 850°C, holding this temperature for 10 h. The cooling rate was 120°C/h until room temperature was reached.

For sample #4, after the initial treatment the gas flow was changed to argon and annealed again at 850°C for 12 h. The precursor was then mixed with HgO (99%, Aldrich) in the nominal stoichiometric quantity. The resulting powder was finally homogenized, pelletized ($m = 3.306$ g, ff = 0.58 g/cm^3) and inserted in the quartz tube of the thermobaric analyzer. The thermal treatment was carried out with a heating rate of 300°C/h up to 700°C, 120°C/h to 860°C, −120°C/h to 850°C and holding this temperature for 10 h. The cooling rate was 120°C/h until room temperature was reached.

For sample #5, after the initial treatment the precursor was then mixed with HgO (99%, Aldrich) in the nominal stoichiometric quantity. The resulting powder was finally homogenized, pelletized ($m = 4.625$ g, ff = 0.75 g/cm^3) and inserted in the quartz tube of the thermobaric analyzer. The thermal treatment was carried out with a heating rate of 300°C/h up to 700°C, 120°C/h to 850°C, −120°C/h to 840°C and holding this temperature for 15 h. The cooling rate was 120°C/h until room temperature was reached. The pressure was measured with the thermobaric analyzer [12] previously calibrated before each synthesis procedure. The temperature was registered with a K-type thermocouple that is in contact with the quartz tube that contains the sample. This setup improves the temperature measurement because it reads the temperature of the sample container and not of the furnace. The pressure and temperature data were recorded with an 1-min interval. The experimental points were registered automatically by a personal computer and the $HgCaO_2$ mass loss was determined by weighting the samples after the annealing.

The X-ray diffraction (XRD) and ac-susceptibility characterization was performed with the final samples in the powder form. The finals products were ground in an agate mortar inside a glove box filled with nitrogen and immediately submitted to XRD. The X-ray powder diffraction experiments (Cu-K_α radiation) were performed in a Rigaku Geigerflex mod. 4053A3 with a chamber sample filled with N_2 gas. The ac susceptibility was measured in a home-made calibrated device ($h_{ac} = 5$ A/m and $\nu = 4.23$ kHz) [13].

3. Results and discussion

3.1. The $HgCaO_2$ formation

Two experimental curves of pressure (P) versus temperature (T) obtained with the TBA sensor corresponding to the $HgCaO_2$ formation are shown in Fig. 1; one of them (sample #a) without Re (HgO + CaO) and the other (sample #e) with Re $[(HgO)_{0.82} + (ReO_2)_{0.18} + CaO]$. The curves were registered during the complete thermal cycle with heating and cooling ramps and the arrows indicate the direction of the thermal treatment. In the heating ramp, for the sample without Re (#a), the pressure presents an exponential-type behavior with the temperature along the whole range of T; however, when Hg is substituted by Re (#e), the P versus T curve presents a complex behavior.

In the cooling process, both curves behave similarly to their respective heating part, although

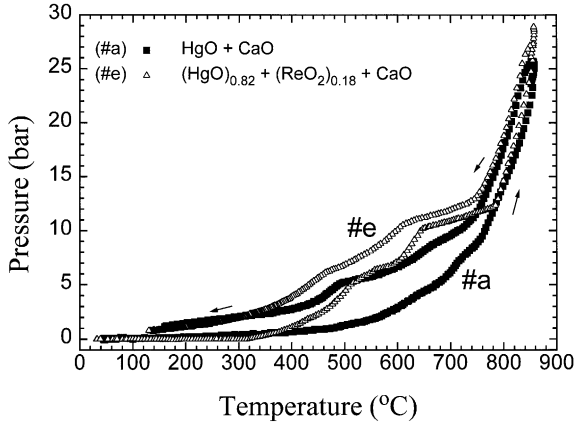

Fig. 1. Pressure versus temperature diagrams of the reactions: #a (HgO + CaO), and #e ($(HgO)_{0.82} + (ReO_2)_{0.18} + CaO$).

the pressures are slightly higher. This occurs because the absorption rate is slowed down due to the Arrhenius-type law controlling the absorption process. In this way, the thermodynamic equilibrium is not exactly reached in the cooling branch because the formation kinetics of a solid from gas during the cooling process is slower than the opposite process in the heating ramp. Consequently, a thermodynamic analysis may not be applied in the cooling curve to produce numerical values for variables such as ΔH and ΔS, but even so, a signature of the existing chemical reaction may be also observed in the cooling process. For example, the cooling curve of sample #e at 600°C displays a slight inflexion that may be attributed to the $HgO_{(s)}$ formation, which is in agreement with the observation of minor amounts of red $HgO_{(s)}$ coating the inner wall of the tube as well as its presence in the sample surface. Moreover, the inflection point in the cooling curves of both samples at about 470°C can be attributed to the condensation of $Hg_{(g)}$, which was observed as droplets inside the capsule.

Fig. 2 shows the normalized XRD patterns of the seven samples with different substitutions of Hg by Re. The results indicate that ReO_2 does not form the compound $Hg_{1-x}Re_xCaO_{2+\delta}$, but it reacts with part of CaO forming the compound $Ca_5Re_2O_{12}$, while the rest of CaO forms $HgCaO_2$. As a consequence, part of HgO does not react, which is confirmed by the direct measurement of the mass of HgO proportion lost by the samples, as shown in Fig. 3.

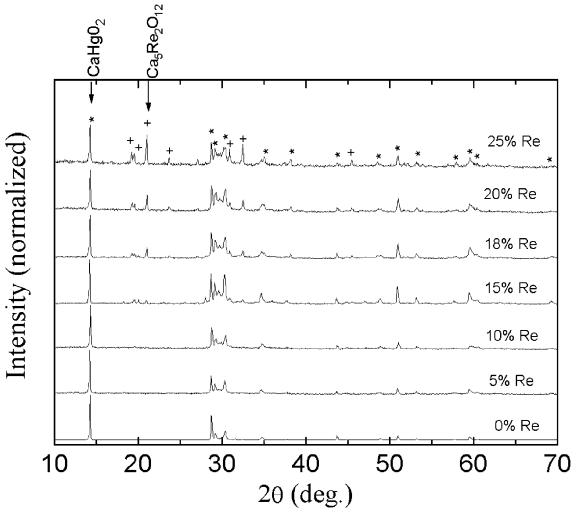

Fig. 2. XRD patterns for seven samples with different substitutions of Hg by Re. When the Re concentration increases, the $HgCaO_2$ amount decreases, improving the $Ca_5Re_2O_{12}$ formation. The maximum intensity reflections, of $HgCaO_2$ and $Ca_5Re_2O_{12}$ are indicated in the figure.

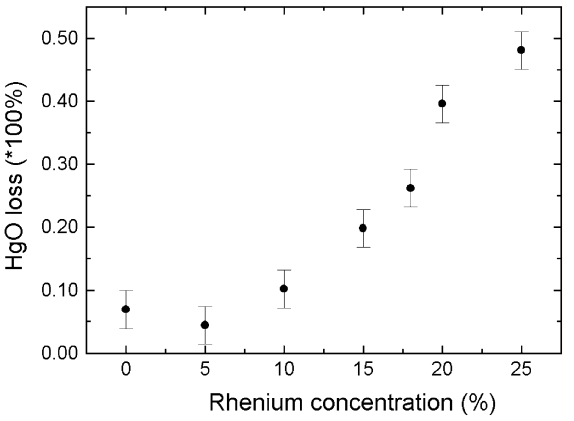

Fig. 3. The perceptual HgO mass loss for seven reactions $[(HgO)_{1-x} + (ReO_2)_x + CaO]$, with different Re concentrations.

A complex behavior of the pressure may be observed in the diagrams, as can be seen in Fig. 1. For a better understanding, we have separated the heating curves into different regions, for several samples, and we discuss the reaction mechanism that operates in each of these intervals.

3.1.1. First region

The first important region is shown in Fig. 4, where are displayed the heating ramps for six different samples up to 600°C. For a better understanding, it was also plotted the theoretical curve of pressure versus temperature of the HgO decomposition

$$2HgO_{(s)} \leftrightarrow 2Hg_{(g)} + O_{2(g)}. \quad (1)$$

The theoretical curve is given by $P = 3\{1/4 \times \exp[-(\Delta H/T - \Delta S)/R]\}^{1/3}$, that can be deduced from the analysis of the decomposition reaction, because its equilibrium constant K depends on the

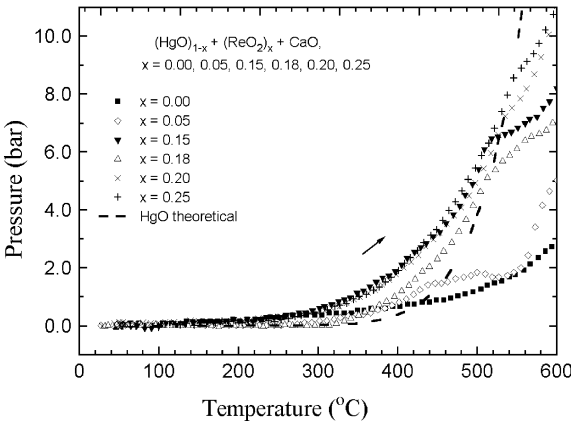

Fig. 4. Heating ramps for six samples doped with Re, up to 600°C, with a theoretical curve for HgO decomposition. The kink pressure occurs always when the HgO decomposition curve intercepts the $HgCaO_2$ curve.

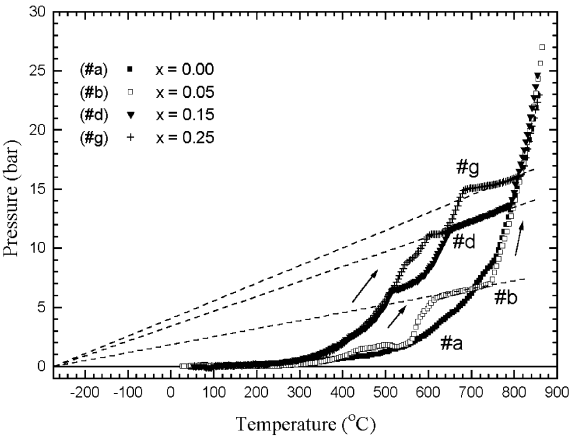

Fig. 5. Pressure versus temperature diagram synthesis for $[(HgO)_{1-x} + (ReO_2)_x + CaO]$ to four different characteristic curves, $x = 0.0, 0.05, 0.15, 0.25$ during heating ramps showing the linear region behavior.

partial pressures of the components (and as a consequence, on the total pressure) through the equation $K = (p_{Hg})^2 p_{O_2} = 4(P/3)^3$, and on the absolute temperature through the equation $\ln K = -\Delta G/RT = -(\Delta H - T\Delta S)/RT$. The values of ΔH and ΔS used in the theoretical expression are reported in the literature [14].

From the analysis of the results, we suggest that when the temperature starts increasing, the total pressure inside the tube, for some samples, is greater than that of the HgO decomposition; when the total pressure of the samples is equal to that of HgO decomposition, the total pressure drops. This occurs because we may assume that ReO_2 reacts with CaO forming the compound $Ca_5Re_2O_{12}$. For that, it was necessary to have more oxygen to form the compound, and oxygen from HgO was then used. We present this interpretation because there is $Hg_{(l)}$ in the sample, and since $Hg_{(l)}$ has a higher vapor pressure than HgO, the initial elevation of pressure must be provoked by the $Hg_{(l)}$ evaporation. The pressure drop occurs always when the pressure of each sample attains the HgO decomposition curve. This suggests that the gas composition is $2Hg_{(g)} + O_{2(g)}$. In this situation the gases are in a proper stoichiometric quantity to react with CaO in order to promote the $HgCaO_2$ formation. The gas–solid reaction can display such pressure drop behavior.

3.1.2. The linear behavior region

The second important region is shown in Fig. 5 and is characterized by a linear behavior between P and T for the samples containing Re. The sample without Re (#a) shows an exponential type behavior. When the HgO is partially changed by ReO_2, the P versus T curve presents an approximate linear behavior for temperatures above 600°C, as can also be seen for samples #b and #d. The behavior changes to an exponential type (and approximately) when each one of these curves reaches the curve for the sample without Re (#a).

The linear behavior for samples doped with 5–18% of Re corresponds to an ideal gas. This suggests that in this linear pressure region occur only a gas expansion, indicating the complete formation of $HgCaO_2$ and $Ca_5Re_2O_{12}$. When the linear region starts the compounds $HgCaO_2$ and $Ca_5Re_2O_{12}$ must have already been formed and the oxygen is completely consumed, remaining the $Hg_{(g)}$ expanding as an ideal gas. This behavior can be understood considering the Gibbs' phase rule [15], which states that the degrees of freedom are given by $F = C + 2 - p$, (where p is the number of phases and C is the number of components). C is given by $C = N - r$, where N is the number of chemical substances and r the number of relationships between them (reactions and stoichiometry ratios).

In the present case, $N = 3(HgCaO_{2(s)}, Hg_{(g)}, Ca_5Re_2O_{12(s)})$, $r = 0$ and $p = 3$ (two solid phases: $Ca_5Re_2O_{12(s)}$ and $HgCaO_{2(s)}$ and one gas phase, $Hg_{(g)}$). Replacing these values in the Gibbs' phase rule we obtain $F = 2$, and this corresponds to a gas expansion.

For sample #b the linear behavior does not change immediately when it reaches the curve of the sample #a, but it remains linear for more 40°C. After this point starts the exponential type behavior, which suggests that Re at low concentrations is a catalyst for the reaction of the $HgCaO_2$.

When the Re concentration is raised above 18–25% there is a change in the beginning of the linear behavior region. In this case the pressure drops slightly and then it shows a proper linear behavior. One possible explanation for this is the increase of Re concentration, which may initially form $Ca_5Re_2O_{12}$, but when the temperature is raised, the Re excess can modify the chemical potential of the $Ca_5Re_2O_{12}$ and part of the compound changes its phase to form other compounds, liberating Ca and O_2 to react with the $Hg_{(g)}$, forming more $CaHgO_2$. In this way the drop in the pressure may be due to the reduction of Hg in the atmosphere.

3.1.3. $HgCaO_2$ decomposition reaction

We may assume that after the linear region, and in the beginning of the exponential type behavior between 750°C and 780°C, the system changes its thermodynamic state and occurs the decomposition reaction

$$HgCaO_{2(s)} \leftrightarrow CaO_{(s)} + Hg_{(g)} + 1/2O_{2(g)}. \qquad (2)$$

Applying the Gibbs' phase rule to the present case, where $N = 5$ $(Hg_{(g)}, O_{2(g)}, CaO_{(s)}, Ca_5\ Re_2O_{12(s)}, HgCaO_{2(s)})$, $r = 2$ $(1 : p_{Hg} = 2p_{O_2}; 2 : Hg + 1/2O_2 + CaO \leftrightarrow HgCaO_2)$ and $p = 4$ (three solid phases: $Ca_5Re_2O_{12(s)}$, $CaO_{(s)}$ and $HgCaO_{2(s)}$; and one gas phase: $Hg_{(g)}$ together with $O_{2(g)}$) we obtain $F = 1$. This corresponds to phase equilibrium.

From the thermodynamic analysis of $HgCaO_2$ at high temperatures, by using the total pressure in the decomposition reaction of $HgCaO_2$ (Eq. (2)) in the heating ramp it is possible to obtain a linear fit when $\ln K = \ln 4(P/3)^3$ is plotted against $1/T$. It

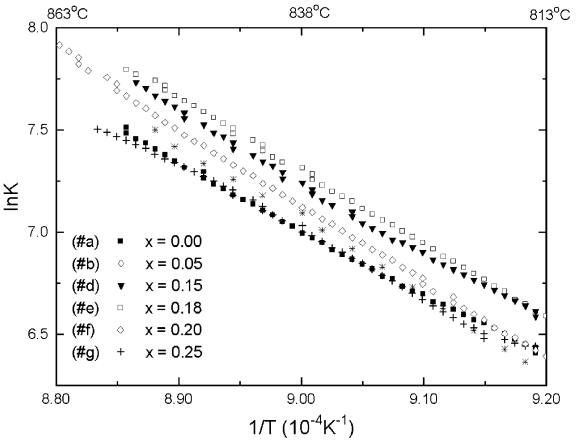

Fig. 6. Plot of $\ln K$ (derived from the measured total pressure) versus $1/T$ for the $HgCaO_2$ synthesis for six samples with different ratio of substitution of HgO by ReO_2.

should be observed that the linearity can only be valid when one solid phase is decomposing. The plots are shown in Fig. 6 for six samples, where it is possible to notice the corresponding linear behavior. These plots help to obtain the enthalpy and entropy of the reaction. Applying the van't Hoff equation, $d\ln K/d(1/T) = -\Delta_d H^0/R$, it was possible to calculate the thermodynamic values such as $\Delta_d H^0$ and $\Delta_d S^0$, to $HgCaO_{2(s)}$ for the dissociation.

Fig. 7 shows the values of $\Delta_d H^0$ and $\Delta_d S^0$ for all samples at 850°C. The enthalpy and entropy of dissociation for $HgCaO_2$ presents a maximum

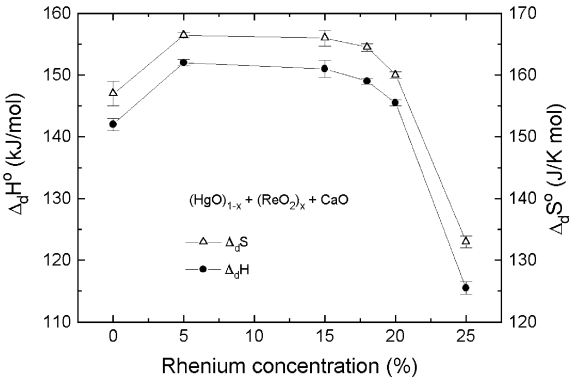

Fig. 7. $\Delta_d H$ and $\Delta_d S$ versus Re concentration diagram at 850°C for $[(HgO)_{1-x} + (ReO_2)_x + CaO]$ reaction with $x = 0.00$, 0.05, 0.15, 0.18, 0.20, 0.25 in the heating ramps.

Table 1
Calculated values of $\Delta_d H$, $\Delta_d S$, using the van't Hoff equation, in the temperature interval $T_f - T_i$ for $HgCaO_2$ decomposition and $\Delta_d G$ for 850°C

% Re	$\Delta_d H$ (kJ/mol)	$\Delta_d S$ (J/K mol)	$T_i - T_f$ (°C)	$\Delta_d G$ (kJ/mol) (850°C)
0	142(1)	157(1)	831–857	−34.3(6.5)
5	152.0(5)	166.5(5)	825–854	−34.9(1.5)
15	151(1.4)	166(1.3)	816–857	−35.4(3.4)
18	149.0(6)	164.5(6)	825–851	−35.7(1.7)
20	145.5(5)	160.0(0)	828–857	−34.2(1.5)
25	116(1)	133(1)	846–858	−33.9(2.5)

between 5% and 15% of Re doping. At this temperature the effect of the entropy value multiplied by T is important to the dissociation of the compounds because it becomes closer to the enthalpy value. In order to understand the Re effect during decomposition it may be better to use the values for Gibbs' free energy. Table 1 presents for each Re concentration the calculated values of $\Delta_d H^0$ and $\Delta_d S^0$ around 850°C and $\Delta_d G^0$ at 850°C for $HgCaO_2$ decomposition. To obtain the Gibbs' free energy of dissociation at 850°C, the equation $\Delta_d G^0 = \Delta_d H^0 - T\Delta_d S^0$ was used, with the values obtained by the van't Hoff equation.

In order to determine the relative stability of each decomposition reaction for samples doped with Re, the Ellingham diagram $\Delta_d G^0$ versus T was used. The $\Delta_d G^0$ values were obtained from the equation $\Delta_d G^0 = -RT \ln K$ and the corresponding diagrams are shown in Fig. 8. The easiest dissociation is given by the lowest $\Delta_d G^0$ value. All the samples present similar behaviors but as the Re concentration increases, the $\Delta_d G^0$ is reduced, attaining a minimum for 18% of Re (−35.7 kJ/mol), and increasing again for higher values of Re concentration. We conclude that the sample doped with 18% of Re has the lowest energy of dissociation, being the easiest to decompose at high temperatures.

3.2. The formation of superconductor $Hg_{1-x}Re_xBa_2Ca_2Cu_3O_{8+\delta}$

After reaching the understanding of the formation mechanisms of the $HgCaO_2$ phase and the

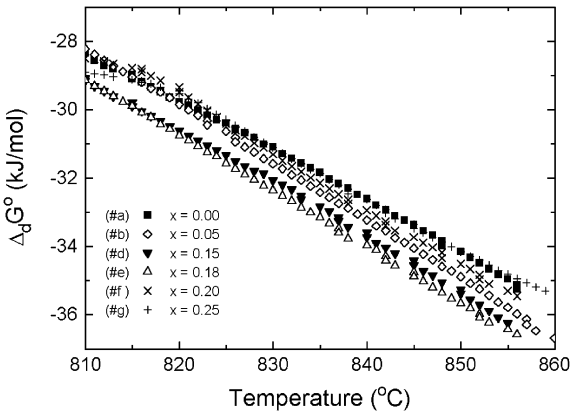

Fig. 8. $\Delta_d G$ versus T diagram for the $HgCaO_2$ synthesis with six samples with different substitutions of HgO by ReO_2.

effects provoked by Re we have decided to investigate the behavior of pressure × temperature for the (Hg,Re)-1223 superconducting phase synthesis and to compare the synthesis parameters.

The samples with different Re concentrations received different heat treatments in order to obtain the phase $n = 3$. The XRD and ac susceptibility measurements confirmed the phase $n = 3$ with $T_c = 133$ K for all samples, cf. Fig. 9. Fig. 10 shows the XRD patterns for two representative samples, one with 15% Re and other without Re. Fig. 11 shows the cell parameters evolution versus Re content. In Ref. [16] we show a more complete study of cell parameters evolution with Re

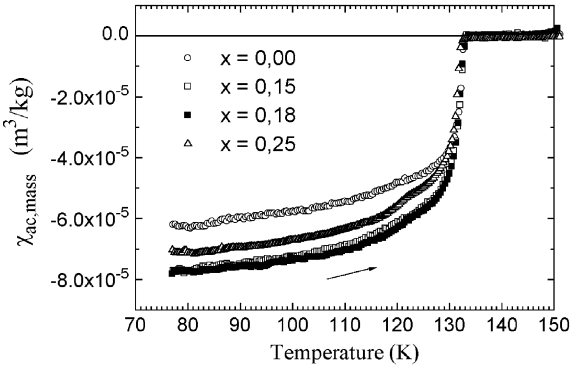

Fig. 9. ac-susceptibility measurements for all samples showing the phase $n = 3$ with $T_c = 133$ K as predominant.

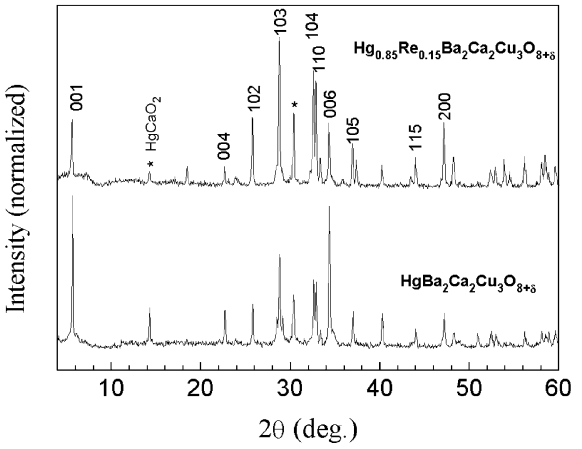

Fig. 10. The XRD patterns for two representative superconducting samples, one with 15% Re and other without Re.

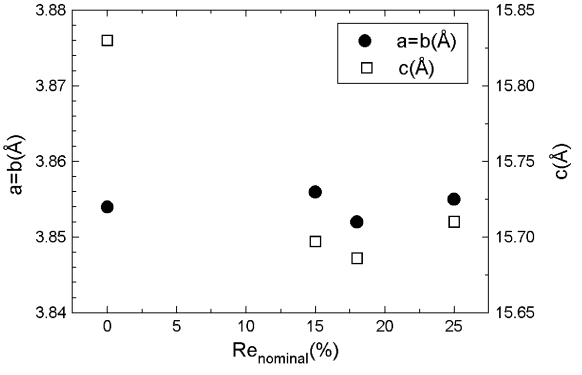

Fig. 11. The cell parameters evolution versus Re content by Rietveld method.

concentration. Fig. 12 shows the diagram P versus T for the five samples and the insert in the figure shows the complete treatment cycle with the heating and cooling branch for the sample #1 ($HgBa_2Ca_2Cu_3O_{8+\delta}$). For a better understanding, the figure shows only the heating branch for the five samples. In this plot it is possible to notice that the sample without Re has a lower synthesis pressure above 770°C. This result is different of the results presented by Xue et al. [9], where they used the N_2 quenching to determine the pressure of Hg during the synthesis of superconductor (Hg,Re)-1223.

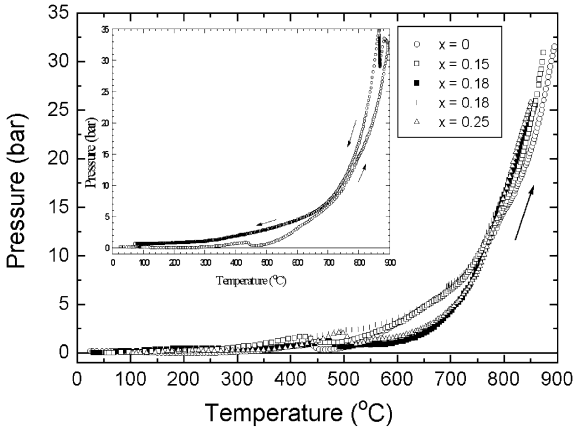

Fig. 12. Pressure versus temperature diagram during heating of the $Hg_{1-x}Re_xBa_2Ca_2Cu_3O_{8+\delta}$ synthesis for samples with $x = 0.00$, 0.15, 0.18 and 0.25. The insert shows the heating and cooling cycles for synthesis of the $HgBa_2Ca_2Cu_3O_{8+\delta}$ superconductor.

An important characteristic of this diagram is the appearance of a kink in the heating ramp at about 440°C. This behavior was experimentally observed in the superconductor synthesis but not in the case of the $HgCaO_2$ synthesis. There is a special interest in the heating process because the increases of the distortion in the curve indicate the appearance of the $CaHgO_2$ in the final synthesis of the composition. When the P–T curve behavior becomes more continuous and the drop in pressure moves to lower temperatures there is a reduction of $CaHgO_2$. The pressure diagram suggests that the reduction of the oxygen content of the precursor and the increase of the partial mercury pressure reduce the $CaHgO_2$ amount, improving the yield of the superconductor formation.

The elevation of pressure before the drop, in this temperature region, is associated with the excess of oxygen in the precursor $Ba_2Ca_2Cu_3O_{7+\delta}$ that interferes in the superconductor formation by decreasing its speed of formation. Since the formation condition of $HgCaO_2$ is essentially via a solid reaction that is occurring continuously, as shown in Fig. 1 for sample #a, a displacement of the peak towards higher temperatures and pressures during the heating ramp increases the quantity of $HgCaO_2$, consequently decreasing the superconductor phase $n = 3$.

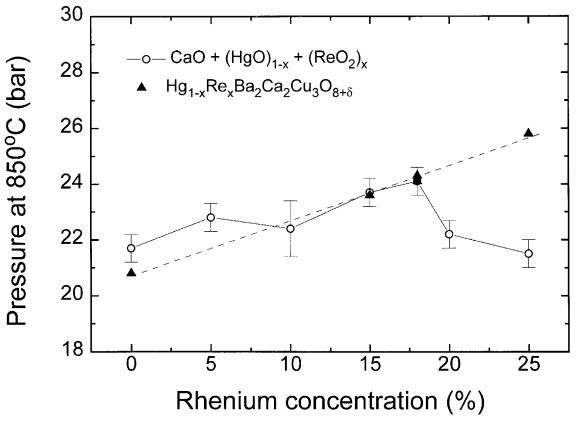

Fig. 13. Pressure at 850°C versus Re concentration for $[(HgO)_{1-x} + (ReO_2)_x + CaO]$ reaction with $x = 0.00$, 0.05, 0.10, 0.15, 0.18, 0.20, 0.25 during heating ramps and $Hg_{1-x}Re_xBa_2Ca_2Cu_3O_{8+\delta}$ synthesis for samples with $x = 0.0$, 0.15, 0.18 and 0.25.

3.3. The competition

The behavior of $P \times T$ for the syntheses of the superconductors and of $HgCaO_2$ are very similar, however with a distinction: the pressure drop which appears during the synthesis of the superconductor around 450°C. To improve the understanding of the competition between the superconductor (Hg,Re)-(1223) and the impurity $HgCaO_2$, it is interesting to compare the pressure at the same temperature during the heating ramp for both cases. Fig. 13 shows the pressure at 850°C during the heating ramp for $HgCaO_2$ and (Hg,Re)-1223 versus Re concentration.

At 850°C, the pressure of $HgCaO_2$ doped with Re shows a maximum for Re concentration at 18%. This behavior seems to be connected with the irregular behavior of the linear part of Fig. 5, sample #g, when the Re concentration was raised above 20%.

The pressure behavior for the superconductor synthesis shows a linear increase when the Re concentration is raised. The pressure for the superconductors synthesis up to 18% of Re concentration, has values that are near or below the values of $HgCaO_2$ doped with Re. It is possible to understand this behavior, since for one certain synthesis be favored it must have a lower pressure than the pressure of competitor phases, and that occurs in all these four samples. According to this point of view, for superconductor syntheses with 20% and 25% of Re or more, the (Hg,Re)-1223 with $n = 3$ phase should not form, because the superconductor synthesis pressure is greater than the pressure of $HgCaO_2$ (Fig. 13). But that not happens, and in fact the $n = 3$ phase is formed, however the sample quality as indicated by ac-susceptibility measurements at 77 K decrease when the Re doping increase above 18% of Re. This unexpected result can be justified by the formation of $Ca_5Re_2O_{12}$ (Fig. 2). At low temperatures Re reacted with Ca, avoiding the formation of $HgCaO_2$ by a portion of the available CaO, and only releasing the Ca to form the superconductor phase at high temperatures. As soon as the Re concentration increases the pressure differences increase, and it is more difficult to maintain the growth of the $n = 3$ phase.

Taking into account only the result of Fig. 13, we could be induced to say that the superconductor $Hg_{0.95}Re_{0.05}Ba_2Ca_2Cu_3O_{8+\delta}$ synthesis should present better results than $Hg_{0.82}Re_{0.18}Ba_2Ca_2Cu_3O_{8+\delta}$, but that was not observed. Up to this moment we have produced several samples with different Re concentrations and the best sample produced was $Hg_{0.82}Re_{0.18}Ba_2Ca_2Cu_3O_{8+\delta}$. This result can be explained by the effect of Re doping in the reaction of $HgCaO_2$. At low concentration like 5%, Re shows a behavior as a catalyst for the $HgCaO_2$ reaction. However, when the concentration of Re is increased, it competes with the Hg to form the compound $Ca_5Re_2O_{12}$. In this way, it decreases the $HgCaO_2$ formation and favors the superconductor synthesis. However, when the Re concentration exceeds 18% the $Ca_5Re_2O_{12}$ becomes unstable allowing the formation of the $HgCaO_2$.

The Re concentration found by EDX analysis shows a different value than the nominal one. The samples with nominal concentration of Re of $x = 0.15$ and 0.18 have a tendency to form a stoichiometry of 1/4 Re and 3/4 Hg in the HgO_δ plane. For a sample with a nominal Re concentration of $x = 0.25$ the Re content reaches $x = 0.28$. A more detailed study about that is described elsewhere [16] and a similar behavior was found by Reder et al. [17].

4. Conclusions

During the reaction between $[(HgO)_{1-x} + (ReO_2)_x + CaO]$ with $0 > x > 0.25$, the ReO_2 does not form the compound $Hg_{1-x}Re_xCaO_{2+\delta}$. In fact, the ReO_2 competes with HgO and reacts with CaO forming the compound $Ca_5Re_2O_{12}$, while the rest of CaO forms $HgCaO_2$. At lower Re concentration ($x \approx 0.05$), $(ReO_2)_x$ behaves as a catalyst for $HgCaO_2$ formation. When the Re concentration is increased the $Ca_5Re_2O_{12}$ formation competes with HgO, reducing the $HgCaO_2$ formation, favoring the superconductor synthesis. However, when the Re concentration exceeds 18%, $Ca_5Re_2O_{12}$ become unstable allowing the $HgCaO_2$ formation.

The TBA allows us to obtain the values of enthalpy, entropy and free energy of dissociation for $HgCaO_2$. The curves of pressure versus Re concentration, Figs. 12 and 13, have revealed that 18% was the "optimum" Re content for our particular set of synthesis conditions. Moreover, since $HgCaO_2$ is produced during the heating step, higher heating rates are beneficial to minimize $HgCaO_2$ formation and improve the Hg-1223 ceramics formation.

The pressure behavior for superconductor synthesis around 850°C suggests a linear increase of the total pressure inside the quartz tube when the Re concentration is raised. This result is opposite to Hg partial pressure behavior found by Xue et al. [9].

Acknowledgements

The authors would like to thank CAPES, CNPq, CST, Finep for the partial support of the work and Dr. Eloi A. Silva Filho for valuable discussions.

References

[1] E.V. Antipov, S.M. Loureiro, C. Chaillout, J.J. Capponi, P. Bordet, J.L. Tholence, S.N. Putilin, M. Marezio, Physica C 215 (1993) 1.
[2] Z.H. He, Q.M. Lin, L. Gao, Y.Y. Sun, Y.Y. Xue, C.W. Chu, Physica C 241 (1995) 211.
[3] B. Raveau, C. Michel, M. Hervieu, A. Maignan, J. Mater. Chem. 5 (6) (1995) 803.
[4] D. Pelloquin, A. Maignan, S. Malo, M. Hervieu, C. Michel, B. Raveau, J. Mater. Chem. 5 (4) (1995) 701.
[5] J. Shimoyama, S. Hahakura, R. Kobayashi, K. Kitazawa, K. Yamafuji, K. Kishio, Physica C 235–240 (1994) 2795.
[6] J.C.L. Chow, P.C.W. Fung, H.M. Shao, C.C. Lam, J. Mater. Res. 11 (6) (1996) 1367.
[7] Y.Y. Xue, Z.J. Huang, X.D. Qiu, L. Beauvais, X.N. Zhang, Y.Y. Sun, R.L. Meng, C.W. Chu, Mod. Phys. Lett. B 7 (1994) 1833.
[8] S. Piñol, A. Sin, A. Calleja, J. Fontcuberta, X. Obradors, F. Espiell, J. Supercond. 11 (1998) 125.
[9] Y.Y. Xue, R.L. Meng, Q.M. Lin, B. Hickey, Y.Y. Sun, C.W. Chu, Physica C 281 (1997) 11.
[10] A. Sin, A.G. Cunha, A. Calleja, M.T.D. Orlando, F.G. Emmerich, E. Baggio-Saitovich, S. Piñol, M. Segarra, X. Obradors, Supercond. Sci. Technol. 12 (1999) 120.
[11] A. Sin, A.G. Cunha, A. Calleja, M.T.D. Orlando, F.G. Emmerich, E. Baggio-Saitovich, S. Piñol, M. Segarra, X. Obradors, Adv. Mater. 10 (1998) 1126.
[12] A.G. Cunha, A. Sin, X. Granados, A. Calleja, M.T.D. Orlando, S. Piñol, X. Obradors, F.G. Emmerich, E. Baggio-Saitovitch, Supercond. Sci. Technol. 13 (2000) 1549.
[13] L. Gomes, M.M.F. Vieira, S.L. Baldochi, N.B. Lima, M.A. Novak, N.D. Vieira Jr., S.P. Morato, A.J.P. Braga, C.L. Cesar, A.A.F.S. Penna, J. Mendes Filho, J. Appl. Phys. 63 (1988) 5044.
[14] Kubaschewski, Metallurgical Thermochemistry, fifth ed., Pergamon International Library, London, 1979.
[15] P.W. Atkins, Physical Chemistry, sixth ed., Oxford University Press, Oxford, 1998.
[16] M.T.D. Orlando, A. Sin, F. Alsina, A.G. Cunha, N. Mestres, A. Calleja, S. Piñol, F.G. Emmerich, L.G. Martinez, M. Segarra, X. Obradors, E. Baggio-Saitovitch, Physica C 328 (1999) 257.
[17] M. Reder, J. Krelaus, L. Schmidt, K. Heinemann, H.C. Freyhart, Physica C 306 (1998) 289.